2024 Panhellenic Conference on Electronics & Telecommunications (PACET) | 979-8-3503-1884-5/24/$31.00 ©2024 IEEE | DOI: 10.1109/PACET60398.2024.10497061

Non-Linear Analysis and Simulation of an Injection Locked Frequency Divider using a Complementary BJT Oscillator

Konstantinos Metaxas, Vassilis Alimisis, Nikolaos P. Eleftheriou and Paul P. Sotiriadis

Department of Electrical and Computer Engineering
National Technical University of Athens, Greece
E-mail: kostismetaxas@yahoo.com, alimisisv@gmail.com, eleftheriou_nikos@hotmail.com, pps@ieee.org

***Abstract*—LC injection-locked frequency dividers offer superior phase noise and power efficiency performance. However, their primary drawback lies in the locking range. This paper presents a nonlinear analysis of the general divide-by-N operation, considering the exponential non-linearity of the BJTs. The analysis employs Harmonic Balance, Bessel functions, and Fourier expansion. The results are applied to the specific case of $N = 2$, demonstrating a close correspondence between the proposed method and the simulated circuit in Cadence IC Suite.**

***Index Terms*—Injection Locked Frequency Dividers, Nonlinear Analysis, Locking Range, Harmonic Balance**

I. Introduction

Frequency dividers are widely used in RF communication applications as key blocks of phase-locked loop (PLL) synthesizers to divide the output frequency by a rational number [1], [2]. Analog injection locked dividers are usually the preferable realization of a frequency divider due to the lower power consumption compared to the digital ones and the low phase noise if they are implemented based on LC resonator [3]. Their main drawback, however, is the limited locking range and further its accurate estimation.

Motivated by the this limitation, this work proposes an analytical method to determine the locking range of a complementary BJT oscillator as depicted in Fig. 1. The proposed model makes use of harmonic balance analysis and Fourier expansion of the exponential non-linearities that arise from the characteristic of the BJT. First, the analysis of the general divide-by-N case is conducted and a general expression for the estimation of the locking range is derived. Next, this analysis is applied to the $N = 2$ case. The experimental validation in the Cadence IC Suite verifies the accuracy of the proposed method.

The remainder of this paper is organized as follows. Section II refers to the circuit under consideration and its mathematical modelling. The proposed non-linear analysis is conducted in Section III, where first the general case of divide-by-N operation is considered and then the general result is applied to the $N = 2$ case. The comparison between the proposed model and the simulation results is described in Section IV. Some concluding remarks are given in Section V.

II. Injection Locked Frequency Divider Circuit and Modelling

The implemented circuit is illustrated in Fig. 1. It consists of two complementary BJT cross-coupled transistors, along with an LC resonator. The input voltage is applied to the base of the tail transistor, and the output is the voltage difference across the capacitor. The mathematical model used for the analysis of the circuit is depicted in Fig. 2, along with its corresponding block diagram which is shown in Fig. 3. It is assumed that the capacitor encompasses all parasitic capacitances of the bipolar transistors, while the resistor R accounts for the ohmic losses of the inductor. The transfer function H applies to the RLC resonator. The non-linear element constituted by the two cross-coupled pairs corresponds to the non-linear function $i = f(v_i, v_o)$.

To derive the expression of the function $i = f(v_i, v_o)$, the currents flowing through the bases of the BJTs are neglected ($\beta \to \infty$). By applying the exponential law for the BJTs and Kirchhoff's laws, we deduce that:

$$
\begin{aligned}
i = f(v_i, v_o) &= -I_q e^{\frac{v_i}{V_T}} \tanh\left(\frac{v_o}{2V_T}\right) = \\
& I_q e^{\frac{v_i}{V_T}} \frac{1 - e^{\frac{v_o}{V_T}}}{1 + e^{\frac{v_o}{V_T}}} = \\
& I_q e^{\frac{v_i}{V_T}} \left(\frac{1}{1 + e^{\frac{v_o}{V_T}}} - \frac{1}{1 + e^{\frac{-v_o}{V_T}}}\right)
\end{aligned} \tag{1}
$$

where I_q is the current of the tail transistor when $v_i = 0$, v_i, v_o and V_T are the input, (differential) output and thermal votlage respectively. The input voltage is described by:

$$v_i = V_T x_1 \cos(\omega_{in} t), \tag{2}$$

and assuming locking, the output voltage is given by:

$$v_o = V_T x_2 \cos(\omega_{out} t + \theta). \tag{3}$$

The input and output frequencies are generally denoted as $\omega_{in}, \omega_{out}$ and the fraction ω_{in}/ω_{out}, which is generally rational, is called rotation number. The normalized amplitudes are described by x_1, x_2 (dimensionless) and θ is the phase difference between the input and output.

For sufficiently small $\Delta\omega = \omega - \omega_0$, where ω_0 is the resonance frequency, which is given by:

$$\omega_0 = \frac{1}{\sqrt{LC}}, \tag{4}$$

the equation $(\omega^2 - \omega_0^2)/\omega$ can be approximated as $2\Delta\omega$ (first order) and hence the frequency responce of the filter is expressed as:

$$H(j\omega) = \frac{H_0}{1 + j2Q\frac{\Delta\omega}{\omega_0}}. \tag{5}$$

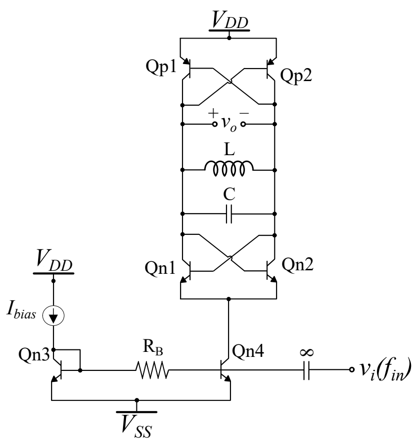

Fig. 1: Injection Locked Divider.

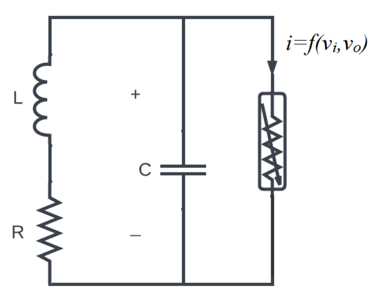

Fig. 2: Mathematical Model of the circuit.

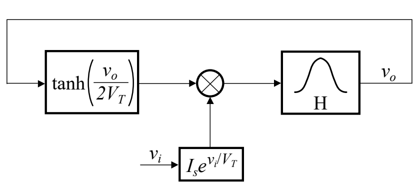

Fig. 3: Block Diagram.

III. Non-Linear Analysis

In this Section, the circuit based on the block diagram shown in Fig. 3 is analysed. A general divide-by-N operation ($N > 1$), which implies the relationship between frequencies $\omega_{in} = N\omega_{out}$, is assumed.

Using (2) and [4] we conclude:

$$e^{v_i/V_T} = e^{x_1 \cos(N\omega_{out}t)} = I_0(x_1) + 2\sum_{n=1}^{\infty} I_n(x_1)\cos(nN\omega_{out}t), \tag{6}$$

where $I_n(x_1)$ is the modified Bessel function of the first kind.

After substituting (3) into (1) and expanding into Fourier series, we obtain:

$$\frac{1}{1 + e^{x_2 \cos(\omega_{out}t + \theta)}} = b_0(x_2) + 2\sum_{n=1}^{\infty} b_n(x_2)\cos(n(\omega_{out}t + \theta)), \quad b_n(x_2) = \frac{1}{2\pi}\int_0^{2\pi} \frac{\cos(n\phi)}{1 + e^{x_2\cos(\phi)}}d\phi. \tag{7}$$

For the second term of (1), let $\gamma = \theta + \pi$, then $-\cos(\omega_{out}t + \theta) = \cos(\omega_{out}t + \gamma)$ and hence

$$\frac{1}{1 + e^{-x_2 \cos(\omega_{out}t + \theta)}} = b_0(x_2) + 2\sum_{n=1}^{\infty} b_n(x_2)\cos(n(\omega_{out}t + \gamma)) = b_0(x_2) + 2\sum_{n=1}^{\infty} b_n(x_2)(-1)^n\cos(n(\omega_{out}t + \theta)), \tag{8}$$

where the coefficients $b_n(x_2)$ are defined in (7). Subtracting (8) from (7) yields:

$$\tanh\left(\frac{v_o}{2V_T}\right) = 4\sum_{m=1}^{\infty} b_{2m-1}(x_2)\cos[(2m-1)\omega_{out}t + (2m-1)\theta]. \tag{9}$$

We note that only odd harmonics appear in the above expansion.

Hence, multiplying (6) with (9), we obtain the expansion of the non-linear function $i = f(v_i, v_o)$,

$$-\frac{i}{I_q} = 4I_0(x_1)\sum_{m=1}^{\infty} b_{2m-1}(x_2)\cos[(2m-1)\omega_{out}t + (2m-1)\theta] + 4\sum_{n=1}^{\infty}\sum_{m=1}^{\infty} I_n(x_1)b_{2m-1}(x_2)[\cos(\alpha_{n,m}(t)) + \cos(\beta_{n,m}(t))], \tag{10}$$

where

$$\alpha_{n,m}(t) = \big(nN - (2m-1)\big)\omega_{out}t - (2m-1)\theta, \tag{11}$$

and

$$\beta_{n,m}(t) = \big(nN + (2m-1)\big)\omega_{out}t + (2m-1)\theta. \tag{12}$$

Assuming that the bandpass filter H rejects all components away from ω_0 and considering that ω_{out} lies sufficiently close to ω_0, the indeces m, n of the terms of the double summation in (10) that pass through the filter must satisfy:

$$nN - (2m-1) = \pm 1 \Rightarrow m = \frac{nN + 1 \mp 1}{2}. \quad (13)$$

If, N, the rotation number, is even, then n is not contrained and traverses all posive integers. If N is odd, then n must be an even integer so that m is also an integer. Hence, we define S as the set of integers in which n belongs. In the case of even N, S is the set of the positive integers, while in the case of odd N, S contains only the even positive integers.

Utilizing (13), the terms of (10) that pass through the filter are given by:

$$\begin{aligned} &4I_0(x_1)b_1(x_2)\cos(\omega_{out}t + \theta) \\ &+ 4\sum_{n\in S}\Big[I_n(x_1)b_{nN-1}(x_2)\cos(\omega_{out}t - (nN-1)\theta) \\ &+ I_n(x_1)b_{nN+1}(x_2)\cos(\omega_{out}t + (nN+1)\theta)\Big]. \end{aligned} \quad (14)$$

By combining (14) with (5), and using phasors, the following complex equation is derived:

$$\begin{aligned} V_T x_2 e^{j\theta} = \frac{H_0 I_q}{1 + 2jQ\frac{\Delta\omega}{\omega_0}}\Big[4I_0(x_1)b_1(x_2)e^{j\theta} + \\ + \sum_{n\in S} 4I_n(x_1)\left(b_{nN-1}(x_2)e^{-j(nN-1)\theta} + b_{nN+1}(x_2)e^{j(nN+1)\theta}\right)\Big], \end{aligned} \quad (15)$$

where $\Delta\omega$ is evaluated at ω_{out}, namely $\Delta\omega = \omega_{out} - \omega_0$. Separating the real and imaginary parts and performing division yields:

$$\Delta x = \frac{N}{D}, \quad (16)$$

where the output-referred normalized locking range denoted by Δx is defined as,

$$\Delta x := \frac{2Q\Delta\omega}{\omega_0}, \quad (17)$$

$$N = \sum_{n\in S} I_n(x_1)\sin(nN\theta)\left[b_{nN+1}(x_2) - b_{nN-1}(x_2)\right], \quad (18)$$

and

$$\begin{aligned} D = b_1(x_2)I_0(x_1) + \\ \sum_{n\in S} I_n(x_1)\cos(nN\theta)\left[b_{nN+1}(x_2) + b_{nN-1}(x_2)\right]. \end{aligned} \quad (19)$$

A. Example: Divide by two

The case $N = 2$ is studied as an illustrative example. Hence, the set S includes all the positive integers. To simplify the analysis and derive an approximate general formula, only the zeroth and first order modified bessel functions are considered. This approximation is reasonable, considering that $I_n(x)$ is decreasing with respect to n and that the output and input voltages are sufficiently small. Further the terms $|b_{nN+1} \pm b_{nN-1}|$ are decreasing with respect to n.

The above observations can be verified by Fig. 4 and Fig. 5 where the first four I_0, I_1, I_2, I_3 modified bessel functions of the first kind and the absolute values of the first four odd indexed coefficients b_1, b_3, b_5, b_7 are shown, respectively. Considering that (16) depends on the product of I_n with $b_{nN+1} \pm b_{nN-1}$, it is clear that higher order terms have negligible contribution. Further, it follows that as x_1 (the injecion voltage) is increased, (16) depends strongly on x_1 and weakly on x_2.

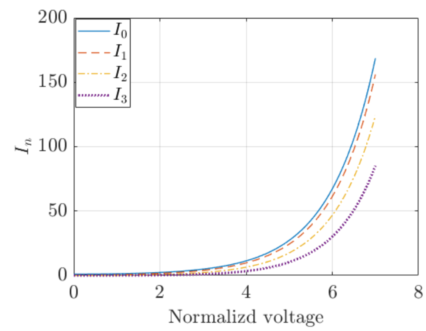

Fig. 4: The first four Bessel functions of the first kind I_0, I_1, I_2, I_3.

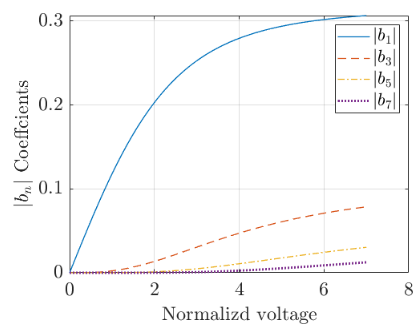

Fig. 5: The first four odd indexed coefficients b_1, b_3, b_5, b_7.

Hence, considering only the terms corresponding to $n = 1$ in the sums of Eq. (19) and (18), (16) becomes:

$$\Delta x = \frac{A\sin(2\theta)}{B + C\cos(2\theta)}, \quad (20)$$

where

$$A = I_1(x_1)(b_3(x_2) - b_1(x_2)), \; C = I_1(x_1)(b_1(x_2) + b_3(x_2)), \quad (21)$$

and

$$B = I_0(x_1)b_1(x_2). \quad (22)$$

The output-referred one-sided normalized locking range, Δx, is maximized when $\cos(2\theta) = -C/B$. The corresponding maximum one-sided input-referred locking range is:

$$\Delta\omega_{\text{max}} = \frac{\omega_0}{Q}\frac{A}{\sqrt{B^2 - C^2}}. \quad (23)$$

Note that the input-referred locking range is twice the output-referred locking range, given that $N = 2$.

IV. Simulation Results and Comparison

The frequency divider in Fig. 1 was simulated for divide-by-2 operation using Cadence IC Suite. The frequency of the unforced oscillator was set to $f_0 = 1GHz$ using $L = 18nH$, $C = 1pF$ and $R = 5\Omega$. The quality factor Q is equal to 26.8.

Simulating the circuit for various input frequencies around 2GHz (given the divide-by-2 operation) and input voltage amplitudes, the output voltage amplitude is extracted and depicted in Fig. 6. As expected, for small input voltages, the output voltage is also small and the locking range (the range of input frequencies for which the output voltage exceeds a threshold of 10mV) is too narrow. An increase in the input voltage results in higher output voltages and a wider locking range. If the input voltage is kept fixed, the output voltage is reduced as the input frequency deviates from 2GHz. It is worth noting the asymmetry, as the output voltage is reduced to smaller values when $f_{in} < 2GHz$ compared to the case when $f_{in} > 2GHz$. Furthermore, the frequency range of operation is wider for $f_{in} < 2GHz$.

Next, Eq. (23) is used to determine the theoretical locking range and compare it with the simulated results. Using the output voltage extracted from the simulation at the maximum and minimum frequencies at which locking occurs, and numerically computing the coefficients b_1 and b_3 through Eq. (7) in MATLAB, we find the one-sided (corresponding to positive and negative deivations from f_0) locking range for various input voltages from Eq. (23). The sum of the one-sided locking ranges, for a given input voltage, equals the theoretical input-referred locking range. Fig. 7 displays both the theoretically derived and simulated results. For small input voltages, as observed in Fig. 7, practically no locking occurs, while Eq. (23) predicts a small value. As the input voltage is increased, the theoretical curve smoothly approximates the simulated one with an error of no more than 4MHz, verifying, further, the stronger dependence on the injection voltage.

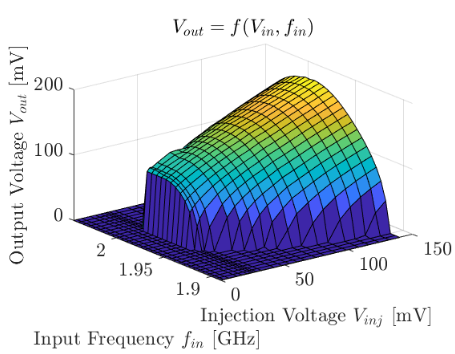

Fig. 6: Output voltage as a function of the input voltage and frequency.

V. Conclusion

A non-linear analysis of the injection-locking characteristics exhibited by a cross-coupled BJT frequency divider operating in the divide-by-N mode is presented. By utilizing Bessel functions and Fourier series, a comprehensive expression encompassing all frequency components generated by the exponential non-linearity of the BJT transistor is derived. The final expression depends on the terms corresponding to harmonics, which provide the fundamental frequency. Applying the analysis to the $N = 2$ case, although the theoretical expression predicts locking for small input voltages, such locking does not actually occur. However, as the input voltage increases, the theoretical curve smoothly approximates to the simulated one with a small error. It effectively conveys, both qualitatively and quantitatively, the dependence of the locking range on the injection voltage.

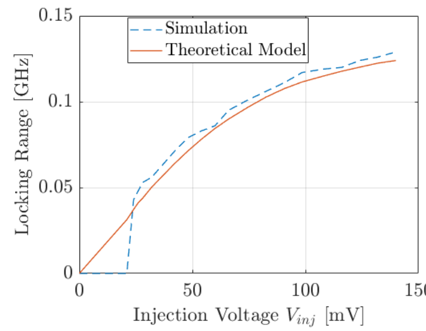

Fig. 7: Theoretical and simulated input-referred locking-range using a thershold of 10mV to determine locking.

References

[1] S. Daneshgar, O. De Feo, and M. P. Kennedy, "Observations concerning the locking range in a complementary differential lc injection-locked frequency divider—part i: Qualitative analysis," *IEEE Transactions on Circuits and Systems I: Regular Papers*, vol. 57, no. 1, pp. 179–188, 2010.

[2] S. Daneshgar and M. P. Kennedy, "A qualitative analysis of a complementary differential lc injection-locked frequency divider based on direct injection," in *2010 IEEE International Symposium on Circuits and Systems (ISCAS)*, 2010, pp. 1531–1534.

[3] Z. Ye, T. Xu, and M. Kennedy, "Locking range analysis for injection-locked frequency dividers," in *2006 IEEE International Symposium on Circuits and Systems (ISCAS)*, 2006, pp. 4 pp.–.

[4] Á. Baricz, *Generalized Bessel Functions of the First Kind*, ser. Generalized Bessel Functions of the First Kind. Springer, 2010, no. 1994.

[5] R. Adler, "A study of locking phenomena in oscillators," *Proceedings of the IRE*, vol. 34, no. 6, pp. 351–357, 1946.

[6] S. Verma, H. Rategh, and T. Lee, "A unified model for injection-locked frequency dividers," *IEEE Journal of Solid-State Circuits*, vol. 38, no. 6, pp. 1015–1027, 2003.

[7] U. Yodprasit and C. Enz, "Nonlinear analysis of a colpitts injection-locked frequency divider," in *Proceedings of the 2003 International Symposium on Circuits and Systems, 2003. ISCAS '03.*, vol. 1, 2003, pp. I–I.

[8] A. Buonomo and A. Lo Schiavo, "A study of injection locking in dual-band cmos frequency dividers," *IEEE Transactions on Circuits and Systems I: Regular Papers*, vol. 64, no. 5, pp. 1225–1234, 2017.

[9] ——, "A nonlinear analysis of differential lc injection-locked frequency dividers," in *2011 20th European Conference on Circuit Theory and Design (ECCTD)*, 2011, pp. 242–245.

[10] P. Maffezzoni, D. D'Amore, S. Daneshgar, and M. P. Kennedy, "Analysis and design of injection-locked frequency dividers by means of a phase-domain macromodel," *IEEE Transactions on Circuits and Systems I: Regular Papers*, vol. 57, no. 11, pp. 2956–2966, 2010.

[11] D. O'Neill, D. Bourket, Z. Ye, and M. Kennedy, "Accurate modeling and experimental validation of an injection-locked frequency divider," in *Proceedings of the 2005 European Conference on Circuit Theory and Design, 2005.*, vol. 3, 2005, pp. III/409–III/412 vol. 3.